Sakarya University Journal of Science

ISSN : 2147-835X
Publisher : Sakarya University

Vol. 28, No. 5, 1047-1058, 2024
DOI: https://doi.org/10.16984/saufenbilder.1515337

Research Article

Investigation of Spintronic Properties of Transition Metal Doped ZnO Thin Films Produced by Sol-Gel Spin Coating

Zafer Gültekin[1*], Cengiz Akay[1], Nuray Altınölçek Gültekin[2]

[1] Bursa Uludag University, Faculty of Science, Department of Physics, Bursa, Türkiye, zafergultekin@uludag.edu.tr, cenay@uludag.edu.tr
[2] Bursa Uludag University, Department of Food Technology, Bursa, Türkiye, altinolcek@uludag.edu.tr
[*]Corresponding Author

ARTICLE INFO

Keywords:
Sol-Gel Spin Coating
DMS Materials
Metal-Oxide Thin Films
ZnO
Contact Angle

Article History:
Received: 12.07.2024
Accepted: 24.09.2024
Online Available: 18.10.2024

ABSTRACT

Transition metal-doped diluted semiconductor materials have attracted significant interest in spintronic applications. In order to investigate the structural, optical, electrochemical, and magnetic properties of these diluted magnetic semiconductors, transition metal-doped ZnO thin films were successfully produced at room temperature using a low-cost sol-gel spin coating technique with the same molar ratios. XRD analyses revealed that all samples adopted the crystal structure of ZnO. Optical measurements indicated high transparency in the visible region for all samples, while electrical measurements confirmed that all samples were n-type semiconductors. Finally, magnetic measurements showed that pure ZnO and Al-doped ZnO exhibited diamagnetic behavior, while Ni and Co doped ZnO displayed magnetic behavior. These results show that Co and Ni-doped ZnO films can be used as diluted magnetic semiconductor materials in spintronic applications.

1. Introduction

Zinc oxide (ZnO) is an n-type semiconductor with a bandgap of 3.37 eV. Its high transparency, electron mobility, stability, and biocompatibility make ZnO suitable for electronic and photonic applications [1-12].

ZnO can be doped with transition metals to enhance its structural, morphological, magnetic, electrical, and optical properties [4,13-16]. For example, doping with elements such as Na, Mg, Fe, Cd, and Mn can alter its optical and structural properties [1, 17-21]. Transition metal doping enhances these properties of ZnO, enabling the production of higher-performance and more durable devices [22]. Under normal conditions, ZnO is diamagnetic, but when doped with Co, it exhibits room temperature ferromagnetism (RTFM) behavior, showing diluted magnetic semiconductor (DMS) characteristics [23]. The presence of RTFM in DMS was first predicted by Dietl et al. [24]. Among all DMS materials, ZnO-based compounds have gained the most attention due to their inherent properties and wide range of applications, especially because they become ferromagnetic when doped with most transition metal elements [12, 25-28].

Additionally, DMS materials are a suitable class of materials for the production of spintronic devices such as spin valve transistors and spin organic light-emitting diodes [29, 30]. Transition metal-doped ZnO thin films have attracted significant interest due to their magnetic properties and performance in spintronic applications. These films offer ideal materials that combine semiconductor and magnetic properties, making them suitable for use in magnetic RAM (MRAM), spintronic devices, sensors, and quantum information processing systems. For example, when transition metals like Fe, Co, and Ni are doped into the ZnO matrix, they enhance the material's room

Cite as: Z. Gültekin, C. Akay, N. Altınölçek Gültekin (2024). Investigation of Spintronic Properties of Transition Metal Doped ZnO Thin Films Produced by Sol-Gel Spin Coating, *Sakarya University Journal of Science*, 28(5), 1047-1058. https://doi.org/10.16984/saufenbilder.1515337

temperature ferromagnetic properties, making it suitable for such applications [31, 32].

Samanta et al. recorded weak DMS behavior at room temperature in Co and Al-doped ZnO prepared by pulsed laser deposition [33]. Nallusamy and Nammalvar reported that the saturation magnetization of ZnO films increased when Ni was added to ZnO [34]. Hadimani and colleagues observed that ZnO gained ferromagnetic properties when doped with Fe, and as the Fe content increased from 0 M to 0.2 M, the magnetic moment rose from 0.01 emu/g to 1.1 emu/g [35]. Qi et al. observed room temperature ferromagnetism in Al-doped ZnO films deposited on glass substrates after annealing in an air atmosphere [36].

Several methods can be used to synthesize ZnO films, including molecular beam epitaxy, RF magnetron sputtering, pulsed laser deposition, spray pyrolysis, chemical vapor deposition, and sol-gel spin coating [37-44]. Among these techniques, the sol-gel spin coating method has been preferred due to its low cost and ease of application [45, 46]. Spin coating is a widely preferred technique for preparing ZnO thin films and offers several advantages over other thin-film production methods. First, spin coating provides a low-cost, rapid production process and allows precise control over film thickness and uniformity. These features are especially advantageous for thin-film transistors and other microelectronic applications. Spin coating is also superior in terms of energy efficiency, as it does not require complex equipment and can be performed at room temperature [47, 48].

Other coating methods are generally performed at high temperatures and under vacuum, which increases energy consumption and production costs. Additionally, these methods can negatively affect the surface roughness and uniformity of the films. Spin coating minimizes such disadvantages and enables high-quality film production at low temperatures [48]. In this study, Al, Ni, and Co-doped ZnO thin films were coated on glass substrates using sol-gel and spin coating methods. These coatings were performed using a spin coating device that we produced ourselves [49]. Al doping improves the electrical conductivity of ZnO by increasing its electron density. This feature is important for optoelectronic applications such as transparent conductive oxides (TCOs).

Additionally, Al doping optimizes ZnO's use in thin-film transistors and microelectronic devices by reducing surface roughness and improving crystalline structure properties [32]. Ni doping imparts magnetic properties to ZnO, resulting in materials that exhibit room temperature ferromagnetic behavior. This is critical for spintronic applications. Ni also increases the magnetic anisotropy of ZnO, thereby enhancing its potential use in magnetic data storage and sensor technologies. Furthermore, adding Ni to ZnO allows for the modification of the material's optical and magnetic properties, enabling the development of multifunctional devices [31]. Co is preferred to impart high Curie temperature and stabilized ferromagnetism to ZnO. Co-doped ZnO exhibits room temperature ferromagnetic properties, making it an ideal material for spintronic devices. Additionally, Co enhances the electronic band structure of ZnO, further improving its optical and magnetic properties, thus increasing its usability in optoelectronic applications [48].

2. General Methods

For the synthesis of transition metal-doped ZnO films, methoxyethanol was used as the solvent, monoethanolamine (MEA) as the stabilizer, and $Zn(CH_3CO_2)_2.2H_2O$ (zinc acetate dihydrate) as the Zn source. Initially, 4.40 g of $Zn(CH_3CO_2)_2.2H_2O$ was dissolved in 50 ml of methoxyethanol at a temperature range of 50-60°C, and stirred at 1000 rpm for 15 minutes. Subsequently, 1.22 g of MEA was added to this mixture and stirred for an additional 20 minutes.

To produce Co-doped ZnO (Co-ZnO), Ni-doped ZnO (Ni-ZnO), and Al-doped ZnO (Al-ZnO), ZnO films were doped with 0.01, 0.02, 0.03, 0.04, 0.05, and 0.1 M of cobalt acetate tetrahydrate $(CH_3COO)_2Co.4H_2O$), nickel acetate tetrahydrate $(Ni(CH_3COO)_2.4H_2O)$, and aluminum nitrate nonahydrate $(Al(NO_3)_3.9H_2O)$. The mixture was then stirred for an additional 15 minutes. A total of 12 different sol-gel solutions were obtained. These solutions were allowed to age for one day before use. After this process,

glass substrates, which were subjected to the cleaning procedure described in Figure 1, were coated with these solutions using spin coating. The coating process was carried out at a speed of 2000 rpm for a duration of 20 seconds. All obtained films were subjected to thermal annealing at 300°C. According to the examinations, the most efficient results were obtained with a doping concentration of 0.03 M.

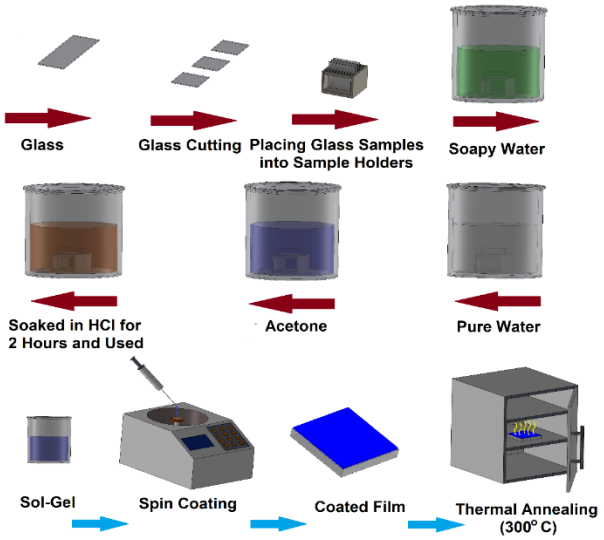

Figure 1. Steps of glass substrate cleaning and sol-gel spin coating process

3. Results and Discussion

The X-ray diffraction (XRD) patterns of ZnO, Co-ZnO, Ni-ZnO, and Al-ZnO thin films are shown in Figure 2. It can be observed that all diffraction peaks exhibit the dominant hexagonal wurtzite structure of ZnO. The diffraction peaks observed at approximately 31°, 33°, 36°, 57°, and 61° correspond to the (100), (002), (101), (102), (110), and (103) planes of ZnO, respectively. The observed diffraction patterns are consistent with the results reported in JCPDS card no: 36-1451 and [1]. The three main peaks corresponding to the (100), (002), and (101) planes of the hexagonal wurtzite structure of ZnO appear more prominent than the other peaks. No additional peaks corresponding to Co, Ni, or Al were observed in the XRD patterns. This result confirms that Co^{2+}, Ni^{2+}, and Al^{3+} are fully incorporated into the ZnO crystal lattice. Similar results have also been reported in [50].

Additionally, the peak position of the (002) plane of ZnO shifted to lower angles after metal doping (this was observed for all three doping metals). This indicates that the lattice dimensions expand with doping, increasing the interplanar distance (d). Larger d-values correspond to smaller 2θ angles. The reason for this is the substitution of Zn atoms in the crystal structure of undoped ZnO with atoms of other elements (in this case, Al, Ni, and Co). The ionic radius of Zn^{+2} is approximately 74 pm, while the ionic radii of Ni^{+2}, Al^{+3} ve Co^{+3} are 69 pm, 53.5 pm, and 61 pm, respectively. These differences lead to changes in the unit cell volume, causing angle shifts.

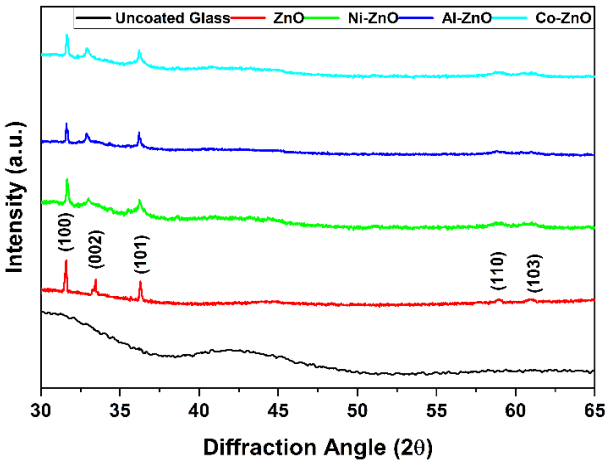

Figure 2. XRD images of uncoated glass and Co, Ni and Al doped ZnO thin films

The average crystallite sizes of the samples were calculated using the Debye-Scherrer formula (1) [1] based on the full width at half maximum (FWHM) of the peaks in the XRD patterns (Table 1).

$$D = \frac{0.9\lambda}{\beta cos\theta} \quad (1)$$

where D is the crystallites size, λ is the X-ray wavelength, θ is the Bragg diffraction angle and β is the full width at half maximum.

A micro strain (ε) of films are calculated from Equation (2) [51, 52].

$$\varepsilon = \frac{\beta \cos\theta}{4} \quad (2)$$

The dislocation density (δ) has been evaluated from Williamson and Smallman's formula (3) [53].

$$\delta = \frac{1}{D^2} \quad (3)$$

The volume of the hexagonal unit cell (*V*) was calculated using Equation (4) [53].

$$V = 0.866a^2c \quad (4)$$

Furthermore, for a given plane with Miller indices (*hkl*) and interplanar spacing ($d_{(hkl)}$), the lattice parameters a=b and c were calculated using Equation (5) [53].

$$\frac{1}{d^2{}_{hkl}} = \frac{4}{3}\left(\frac{h^2 + hk + k^2}{a^2}\right) + \frac{l^2}{c^2} \quad (5)$$

Table 1. Results calculated from XRD data

Material	Lattice Parameters		D (nm)	V (Å^3)	ε (10^{-4})	δ (10^{14}) (m^2)
	a=b (nm)	c (nm)				
ZnO	0.327	0.506	68	46.86	5.1	2.2
Co-ZnO	0.327	0.514	55	47.14	6.3	3.3
Ni-ZnO	0.327	0.509	58	47.32	6.0	3.0
Al-ZnO	0.327	0.511	45	47.60	7.7	4.9

SEM analysis was conducted to gain a detailed understanding of the surface morphology. Figure 3 shows the SEM images of ZnO and Co, Ni, and Al-doped ZnO thin films. The SEM image of pure ZnO (a) exhibits a quite smooth and homogeneous surface structure. The grain boundaries are distinct, and it is evident that the ZnO crystals have grown in a well-ordered manner. The grain sizes are relatively uniform and similar in shape and size, reflecting the typical orderly crystal structure of ZnO. The SEM image (b) of Al-doped ZnO reveals a significantly more homogeneous and smoother structure compared to undoped ZnO. This doping process appears to have reduced the granular features on the surface, resulting in a more compact surface formation.

The integration of aluminum atoms into the ZnO crystal lattice has led to a decrease in surface roughness, creating a more orderly structure at the microscopic level. This homogeneous surface morphology is particularly important for optoelectronic applications, as a smoother surface can enhance light propagation and improve device efficiency. The SEM image of Ni-doped ZnO (c) features a very fine and homogeneous surface structure. The grain boundaries are not as distinct as those in pure ZnO, but the surface appears smoother and finer. The addition of Ni has reduced the grain size of ZnO, leading to the formation of a finer and more uniform structure. The SEM image of Co-doped ZnO (d) has a much finer surface structure compared to ZnO and other doped films. The surface is quite smooth, and the grain boundaries are not distinct. The lack of distinct grain boundaries indicates the presence of very small-sized crystals. This suggests that Co has integrated well into the ZnO structure without creating significant crystal defects.

The grain sizes obtained from the SEM images were added to Table 2. Overall, the results are consistent with the crystallite sizes obtained from the XRD patterns.

Figure 4 shows the contact angle (CA) plots of ZnO and Co, Ni and Al-ZnO films. These values are recorded in Table 2. Besides SEM analysis, surface morphology (roughness) can also be indirectly determined from surface contact angle measurements [54]. The variation in contact angle is greatly influenced by the morphology of the film surface, particularly its roughness [55, 56]. A contact angle of less than 90° between a liquid droplet and a solid surface indicates that the surface is hydrophilic.

When a water droplet contacts a film surface, micro- and nanoscale roughnesses and valleys on the surface play an important role. These valleys can trap air molecules and prevent the water droplet from directly contacting the surface, creating an air barrier on the surface and the surface becomes more hydrophobic [57]. ZnO film exhibits weak hydrophilic character with a surface contact angle value of 74°, while Co, Ni and Al doped ZnO films exhibit stronger hydrophilic characters with contact angle values of 17.5°, 10° and 22°, respectively. The increase or decrease in the contact angle is due to the

increase or decrease in the surface roughness of the film, respectively [58]. The results are consistent with the SEM images.

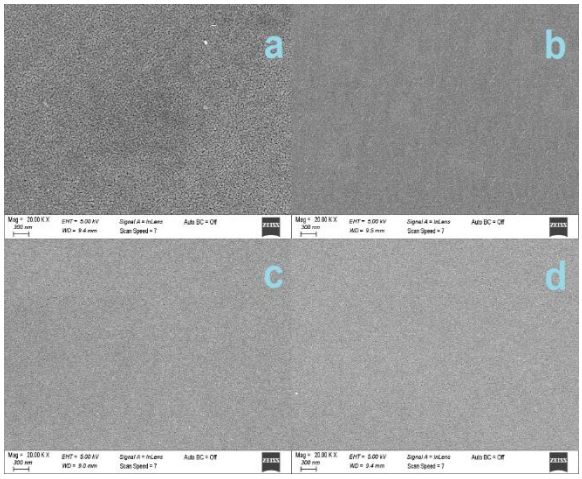

Figure 3. SEM images of thin films. a,b,c and d represent ZnO, Al-ZnO, Ni-ZnO and Co-ZnO, respectively.

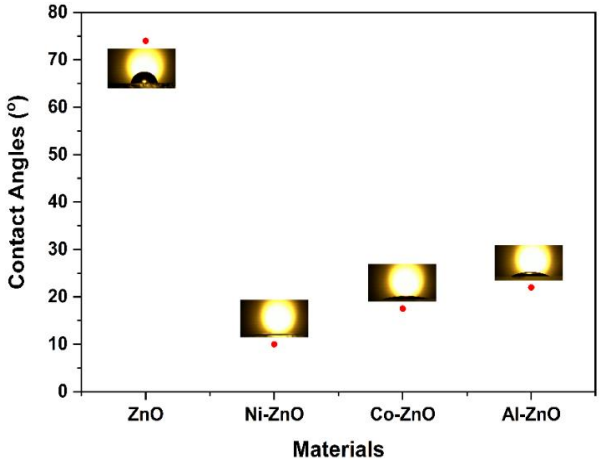

Figure 4. Contact angles of ZnO and Co, Ni and Al doped ZnO thin films

Additionally, the total surface free energies (γ_s) of all films were calculated and added to Table 2. A surface with high surface free energy enables better adhesion of the coating material and facilitates the formation of a more homogeneous coating layer. The surface free energies of Co, Ni, and Al-doped ZnO films are higher than that of undoped ZnO.

Table 2. Results from SEM and contact angle

Material	Grain Size (nm)	CA (°)	γ_s (mN/m)
ZnO	~60	74	59
Co-ZnO	<45	18	143
Ni-ZnO	<45	10	139
Al-ZnO	<45	22	135

The I-V characteristics of ZnO and Co, Ni, and Al-doped ZnO films at room temperature are illustrated in Figure 5. The linearity of the I-V graphs for all samples indicates that the films exhibit ohmic behavior. The resistivities of the films were determined using Equation (6) [51].

$$\rho = \frac{\pi t}{\ln 2}\left(\frac{V}{I}\right) \quad (6)$$

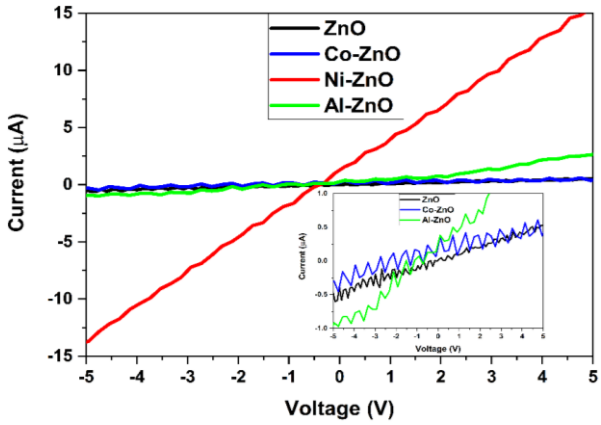

Figure 5. I-V graph of ZnO and Co, Ni and Al doped ZnO thin films

Here, t is the thickness of the thin film, and $(\pi/ln\ 2)\times(V/I)$ represents the sheet resistance (R_{sh}). The calculated resistivity values (ρ) are listed in Table 3. After doping with Co, Al, and especially Ni, the conductivity increased compared to undoped ZnO. This can be attributed to the reduced presence of cracks and agglomerations on the film surfaces, which could otherwise impede electron flow. This is compatible with SEM measurements. Additionally, the increased conductivity indicates better crystallization in the doped films. The increase in carrier concentration (N_s) due to doping also contributes to the enhanced conductivity (Table 3).

Figure 6 shows the optical transmittance spectra of ZnO and Co, Ni, and Al-doped ZnO films. The optical properties of ZnO and ZnO films modified with dopants are closely related to the material's microstructural and crystallographic structure, which can be elucidated through XRD (X-ray diffraction) and SEM (scanning electron microscopy) analyses. Optical transmittance is a significant parameter that emerges during the interaction of a material with light. This property is especially critical in semiconductors like ZnO with a wide bandgap, as it determines the material's potential applications.

ZnO's wide bandgap (approximately 3.41 eV) provides high transparency in the optical transmittance spectrum, particularly in the visible light region. The XRD pattern shows that the crystal structure of ZnO is well-defined, with distinct diffraction peaks. This crystal structure maintains a wide optical bandgap, resulting in high optical transmittance. The sharp and narrow peaks observed in the XRD pattern of ZnO indicate minimal crystal defects, which allow for orderly optical transitions.

The addition of dopants such as Ni, Al, and Co to ZnO significantly alters its optical properties. In Ni-ZnO and Al-ZnO films, shifts and broadening of the peaks in the XRD patterns suggest that dopants integrate into the crystal structure, leading to phase mixtures and crystal distortions. These distortions cause the bandgap energy to narrow, resulting in red shifts in the optical spectrum. Consequently, the lower optical transmittance observed in these materials, especially in the UV region, can be attributed to increased absorption. SEM images support this observation; the irregularities and morphological disruptions seen on the surfaces of Ni-ZnO and Al-ZnO films cause increased scattering of light on the surface, reducing optical transmittance.

On the other hand, Co-ZnO films exhibit relatively sharp and well-defined peaks in XRD patterns, indicating that the crystal structure is not significantly disturbed by Co dopants, allowing ZnO to maintain its wide bandgap. SEM images of Co-ZnO films show a homogeneous and smooth surface structure, which minimizes light scattering and results in high optical transmittance. The stabilization of ZnO's crystal structure by Co dopants enables the optical bandgap to remain wide, thereby achieving high transmittance across a broad wavelength range.

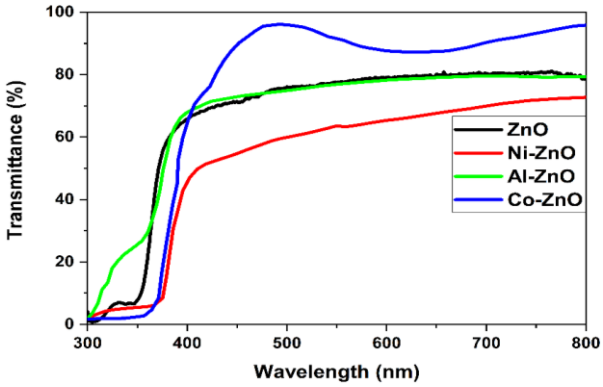

Figure 6. Optical transmittance spectrum of ZnO and Co, Ni and Al doped ZnO thin films

Table 3. Carrier density (N_s), flat band potential (V_{fb}), bandgap and resistivity of materials

Material	N_s (m^{-3})	V_{fb} (V)	Band gap (eV)	ρ (Ω.cm)
ZnO	$1.93x10^{18}$	0.38	3.41	1716
Co-ZnO	$5.41x10^{18}$	0.30	3.26	1320
Ni-ZnO	$5.17x10^{18}$	0.33	3.11	46
Al-ZnO	$4.95x10^{18}$	0.31	3.19	394

The optical energy range E_g of Co, Ni and Al-ZnO thin films was found using the absorption spectra defined by equation (7) and recorded Table 3:

$$\alpha h\upsilon = B\left(h\upsilon - E_g\right)^n \quad (7)$$

α is the absorption coefficient, υ is the frequency of the incident photon, B is a constant and h is Planck's constant [23]. Figure 7 summarizes the band gap obtained for ZnO and Co, Ni and Al doped ZnO thin films. It can be seen from the figure that the ZnO compound has a very large energy range, consistent with the literature [59-61]. Semiconductors like ZnO with bandgaps of this magnitude are optically transparent in the visible region, making them suitable for applications involving short-wavelength light [62].

Transition metals disrupt the structural integrity of the host ZnO cell/crystal, causing band narrowing. When the host ZnO compound is doped with transition metals, the dopant ions replace the Zn ions, changing the ZnO lattice structure. This change in the lattice structure is due to the radius difference of the dopant ions. The change of the graphs is due to the change of these lattice parameters. In the same graph, the x-axis intersection points of the slopes give the

values of the optical energy range of ZnO thin films. The energy ranges of these three ZnO films doped with transition metals correspond to the ultraviolet region.

Figure 8 shows the Mott-Schottky plots for ZnO and Co, Ni, and Al-doped ZnO films. In Mott-Schottky analysis, the slope of the plots provides insights into the carrier density of the films. A positive slope typically signifies that the films behave as n-type semiconductors, where electrons are the majority carriers.

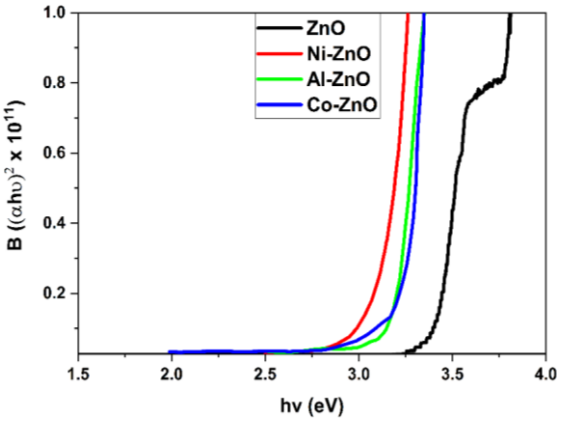

Figure 7. Band gap of ZnO and Co, Ni and Al doped ZnO thin films

Moreover, the intersection points of the Mott-Schottky curves with the x-axis yield the flat band potential (V_{fb}). The carrier densities and flat band potentials obtained from the plots were recorded in Table 3.

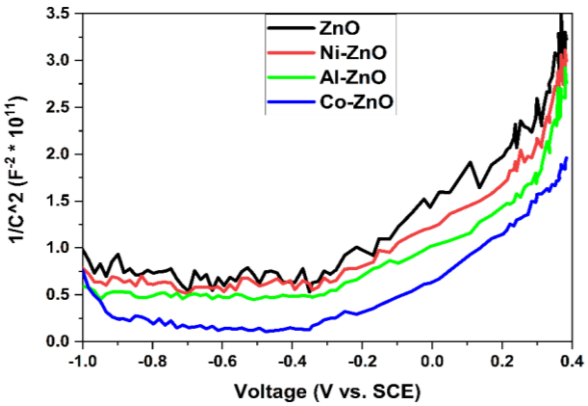

Figure 8. Mott-Schottky graph of ZnO and Co, Ni and Al doped ZnO thin films

The magnetic properties of Co, Ni, and Al-doped ZnO thin films were investigated at room temperature using a vibrating sample magnetometer (VSM). Figure 9 shows the VSM results of ZnO semiconductors doped with Al, Ni, and Co metals. The ZnO sample (inner part in Figure 9) exhibits diamagnetic properties. The figure shows that the Al-doped ZnO semiconductor film behaves diamagnetically similar to ZnO, whereas Ni and Co-doped ZnO semiconductors acquire magnetic properties. Particularly, a rapid increase in the magnetic moment at small magnetic field values (< ±100 Oe) indicates that Ni and especially Co doped ZnO materials exhibit superparamagnetic behaviour [63]. Superparamagnetism is the condition where magnetic particles at the nanoscale exhibit random orientations without interacting with each other.

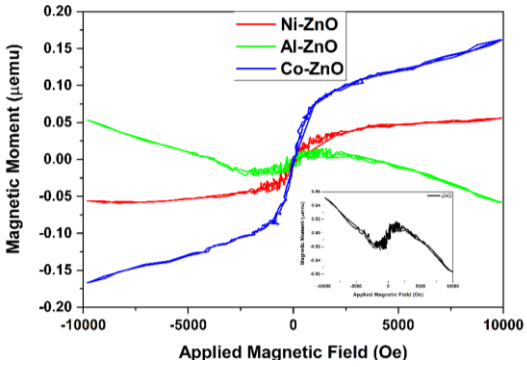

Figure 9. VSM graph of ZnO and Co, Ni and Al doped ZnO thin films

The behavior of DMS is based on the magnetic, optical, and structural changes resulting from the modification of ZnO with magnetic dopants such as Ni, Al, and Co. XRD data indicate that the ZnO matrix retains its wurtzite structure, though the dopants cause slight modifications in the crystal structure. This crystal structure provides a suitable environment for strong ferromagnetic interactions, such as RKKY (Ruderman-Kittel-Kasuya-Yosida) or Zener-type interactions. The highest magnetic moment observed in Co-ZnO on the Figure 9 suggests strong ferromagnetic interaction between dopant ions, attributed to spin alignment between Co ions.

Grain size and defects also contribute to this ferromagnetic behavior; smaller grain sizes and defects can enhance ferromagnetism by increasing the localization of free carriers. The formation of secondary phases (e.g., CoO or NiO) can also support ferromagnetic behavior, as these phases increase the carrier density within the ZnO matrix (Table 3), thereby enhancing ferromagnetic interactions. These findings indicate that ZnO-based DMS materials hold

potential for spintronic applications, with ferromagnetism in these materials being closely related to the type of dopant, carrier density, grain size, and defects.

4. Conclusion

The spin coating technique involves the uniform deposition and production of thin films by spinning the substrate and thin film solution at a certain angular speed. Using this technique, Ni, Al, and Co-doped ZnO films were produced in our laboratory. Our structural analyses revealed that all doped films adopted the crystal structure of ZnO, with no external crystalline phase observed. Optical measurements indicated that each sample exhibited high transparency in the visible region, with band gaps ranging from 3.11 to 3.41 eV. Electrical analysis demonstrated that each semiconductor was of n-type, with carrier concentrations in the range of 1018 m^{-3}. Magnetic measurements showed that pure ZnO and Al-doped ZnO exhibited diamagnetic properties, while Ni and Co-doped ZnO displayed superparamagnetic behaviour. Our results were generally consistent with previous studies reported in the literature. Ni and Co doped ZnO materials produced in our study could be utilized as diluted magnetic semiconductors in spintronic applications.

Article Information Form

Funding
This study was supported by Bursa Uludağ University Scientific Research Projects Commission. Project Code, FHIZ-2023-1608.

Authors' Contribution
The authors contributed equally to the study.

The Declaration of Conflict of Interest/ Common Interest
No conflict of interest or common interest has been declared by the authors.

The Declaration of Ethics Committee Approval
This study does not require ethics committee permission or any special permission.

The Declaration of Research and Publication Ethics
The authors of the paper declare that they comply with the scientific, ethical and quotation rules of SAUJS in all processes of the paper and that they do not make any falsification on the data collected. In addition, they declare that Sakarya University Journal of Science and its editorial board have no responsibility for any ethical violations that may be encountered, and that this study has not been evaluated in any academic publication environment other than Sakarya University Journal of Science.

References

[1] Z. Gültekin, M. Alper, M. C. Hacıismailoğlu, C. Akay, “Effect of Mn doping on structural, optical and magnetic properties of ZnO films fabricated by sol–gel spin coating method,” Journal of Materials Science: Materials in Electronics, vol. 34, no. 438, pp. 1-14, 2023.

[2] C. D. Bojorge, H. R. Canepa, U. E. Gilabert, D. Silva, E. A. Dalchiele, R. E. Marotti, "Synthesis and optical characterization of ZnO and ZnO nanocrystalline films obtained by the sol–gel dip-coating process," Journal of Materials Science: Materials in Electronics, vol. 18, no. 10, pp. 1119-1125 2007.

[3] M. Smirnov, C. Baban, G. I. Rusu, "Structural and optical characteristics of spin-coated ZnO thin films," Applied Surface Science, vol. 256, pp. 2405-2408, 2010.

[4] N. Siregar, J. H. Panggabean, "The effect of spin coating speed on structural and optical properties of ZnO and ZnO/dye thin films synthesized by sol-gel spin coating method," Journal of Physics: Conference Series, Canada, 2021, pp. 1-6.

[5] D. M. Bagnall, Y. Chen, Z. Zhu, T. T. T. Tao, S. Koyama, M. T. Shen, T. Goto, "Synthesis and optical characterization of ZnO nanocrystalline films," Applied Physics Letters, vol. 70, pp. 2230, 1997.

[6] S. J. Pearton, C. R. Abernathy, M. E. Overberg, G. T. Thaler, D. P. Norton, N. Theodoropoulou, A. F. Hebard, Y. D. Park, F. Ren, J. Kim, L. A. Boatner, "ZnO thin films: Synthesis and properties," Journal of Applied Physics, vol. 93, no. 1, pp. 1-13, 2003.

[7] D. C. Look, D. C. Reynolds, C. W. Litton, R. L. Zones, D. B. Eason, G. Conwell, "Structural and optical properties of ZnO films," Applied Physics Letters, vol. 81, pp. 1830-1832, 2002.

[8] C. Liu, F. Yiu, H. Morkoc, "Structural and optical properties of ZnO thin films," Journal of Materials Science: Materials in Electronics, vol. 16, pp. 557-597, 2005.

[9] K. Samanta, P. Bhattacharya, R. S. Katiyar, W. Iwamoto, P. G. Paglius, C. Rettori, "Photoluminescence properties of Cd doped ZnO films," Physical Review B: Condensed Matter and Materials Physics, vol. 73, pp. 245213, 2006.

[10] P. Kumari, K. P. Misra, S. Chattopadhyay, S. Samanta, "A brief review on transition metal ion doped ZnO nanoparticles and its optoelectronic applications," Materials Today: Proceedings, vol. 43, pp. 3297-3302, 2021.

[11] A. Badawi, M. G. Althobaiti, E. E. Ali, S. S. Alharthi, A. N. Alharbi, "A comparative study of the structural and optical properties of transition metals (M= Fe, Co, Mn, Ni) doped ZnO films deposited by spray-pyrolysis technique for optoelectronic applications," Optical Materials, vol. 124, pp. 112055-112062, 2022.

[12] A. Murtaza, W. L. Zuo, X. Song, A. Ghani, A. Saeed, M. Yaseen, S. Yang, "Robust ferromagnetism in rare-earth and transition metal co-doped ZnO nanoparticles for spintronics applications," Materials Letters, vol. 310, pp. 131479, 2022.

[13] Z. Ye, H. He, L. Jiang, "Co-doping: An effective strategy for achieving stable p-type ZnO thin films," Nano Energy, vol. 52, pp. 527-540, 2018.

[14] D. Anbuselvan, S. Nilavazhagan, A. Santhanam, N. Chidhambaram, K. V. Gunavathy, T. Ahamad, S. M. Alshehri, "Room temperature ferromagnetic behavior of nickel-doped zinc oxide dilute magnetic semiconductor for spintronics applications," Physica E, vol. 129, pp. 114665, 2021.

[15] A. F. Fathima, R. J. Mani, M. M. Roshan, K. Sakthipandi, "Enhancing structural and optical properties of ZnO nanoparticles induced by the double co-doping of iron and cobalt," Materials Today: Proceedings, vol. 49, pp. 2598-2601, 2022.

[16] N. Ali, B. Singh, V. Ar, S. Lal, C. S. Yadav, K. Tarafder, S. Ghosh, "Ferromagnetism in Mn-doped ZnO: a joint theoretical and experimental study," The Journal of Physical Chemistry C, vol. 125, no. 14, pp. 7734-7745, 2021.

[17] D. Akcan, A. Gungor, L. Arda, "Structural and optical properties of Na-doped ZnO films," Journal of Molecular Structure, vol. 1161, pp. 299-305, 2018.

[18] K. Verma, B. Chaudhary, V. Kumar, V. Sharma, M. Kumar, "Investigation of structural, morphological and optical properties of Mg: ZnO thin films prepared by sol-gel spin coating method," Vacuum, vol. 146, pp. 524-529, 2017.

[19] B. P. Kafle, S. Acharya, S. Thapa, S. Poudel, "Structural and optical properties of Fe-doped ZnO transparent thin films," Ceramics International, vol. 42, no. 1, pp. 1133-1139, 2016.

[20] B. J. Zheng, W. Hu, "Photoluminescence properties of Cd doped ZnO films obtained

by pulsed laser deposition," Advanced Materials Research, vol. 680, pp. 70-74, 2013.

[21] H. Sun, S. C. Chen, C. H. Wang, Y. W. Lin, C. K. Wen, T. H. Chuang, M. J. Dai, "Electrical and magnetic properties of (Al, Co) co-doped ZnO films deposited by RF magnetron sputtering," Surface and Coatings Technology, vol. 359, pp. 390-395, 2019.

[22] Ü. Özgür, Ya. I. Alivov, C. Liu, A. Teke, M. A. Reshchikov, S. Doğan, V. Avrutin, S.-J. Cho, H. Morkoç, "A comprehensive review of ZnO materials and devices, " Journal of Applied Physics, vol. 98, no. 4, pp. 041301, 2005.

[23] N. Abirami, A. M. S. Arulanantham, K. S. J. Wilson, "Structural and magnetic properties of cobalt doped ZnO thin films deposited by cost effective nebulizer spray pyrolysis technique," Materials Research Express, vol. 7, no. 2, pp. 2020, 2020.

[24] T. Dietl, H. Ohno, F. Matsukura, J. Cibert, D. Ferrand, "ZnO: A ferromagnetic semiconductor," Science, vol. 287, pp. 1019, 2000.

[25] K. Sato, H. Katayama-Yoshida, "Theory of room-temperature ferromagnetism in ZnO-based magnetic semiconductors," Japanese Journal of Applied Physics, vol. 39, pp. L555, 2000.

[26] K. Sato, H. Katayama-Yoshida, "Theory of room-temperature ferromagnetism in ZnO-based magnetic semiconductors (II)," Japanese Journal of Applied Physics, vol. 40, pp. L334, 2001.

[27] Q. Q. Gao, Q. X. Yu, K. Yuan, X. N. Fu, B. Chen, C. X. Zhu, H. Zhu, "Influence of annealing atmosphere on room temperature ferromagnetism of Mn-doped ZnO nanoparticles," Applied Surface Science, vol. 264, pp. 7-10, 2013.

[28] X. Liu, F. Lin, L. Sun, W. Cheng, X. Ma, W. Shi, "Doping concentration dependence of room-temperature ferromagnetism for Ni-doped ZnO thin films prepared by pulsed-laser deposition," Applied Physics Letters, vol. 88, no. 6, pp. 062503, 2006.

[29] M. Benali Kanoun, S. Goumri-Said, A. Manchon, U. Schwingenschlögl, "Ferromagnetism carried by highly delocalized hybrid states in Sc-doped ZnO thin films," Applied Physics Letters, vol. 100, no. 22, pp. 222504, 2012.,

[30] D.P. Norton, S. J. Pearton, J. M. Zavada, W. M. Chen, I. A. Buyanova, "Ferromagnetism in ZnO Doped with Transition Metal Ions," First Edition, C. Jagadish, S. Pearton, Elsevier Science Ltd, 2006, pp. 555-576.

[31] A. Janotti, C. G Van de Walle, "Fundamentals of zinc oxide as a semiconductor, " Reports on Progress in Physics, vol. 72, no. 12, pp. 126501, 2009.

[32] C. G. Jin, Y. Gao, X. M. Wu, M. L. Cui, L. J. Zhuge, Z. C. Chen, B. Hong, "Structural and magnetic properties of transition metal doped ZnO films," Thin Solid Films, vol. 518, no. 8, pp. 2152-2156, 2010.

[33] K. Samanta, P. Bhattacharya, J. G. S. Duque, W. Iwamoto, C. Rettori, P. G. Pagliuso, R. S. Katiyar, "Optical and magnetic properties of $Zn_{0.9-x}Co_{0.1}O:Al_x$ thin films," Solid State Communications, vol. 147, no. 7-8, pp. 305-308, 2008.

[34] S. Nallusamy, G. Nammalvar, "Enhancing the saturation magnetisation in Ni doped ZnO thin films by TOPO functionalization," Journal of Magnetism and Magnetic Materials, vol. 485, pp. 297-303, 2019.

[35] P. L. Hadimani, S. S. Ghosh, A. Sil, "Preparation of Fe doped ZnO thin films and their structural, magnetic, electrical characterization," Superlattices and Microstructures, vol. 120, pp. 199-208, 2018.

[36] Y. K. Qi, J. J. Gu, L. H. Liu, H. Y. Sun, "Annealing effects on structural and magnetic properties of Al doped ZnO thin films," Advanced Materials Research, vol. 239, pp. 2835-2838, 2011.

[37] Z. Changzheng, "Effect of the oxygen pressure on the microstructure and optical properties of ZnO film prepared by laser molecular beam epitaxy," Physica B: Condensed Matter, vol. 404, pp. 404-408, 2009.

[38] T. Minami, H. Nanto, S. Takata, "Optical properties of aluminum doped zinc oxide thin films prepared by RF magnetron sputtering," Japanese Journal of Applied Physics, vol. 24, pp. L781, 1985.

[39] B. L. Zhu, "Low temperature annealing effects on the structure and optical properties of ZnO films grown by pulsed laser deposition," Vacuum, vol. 84, pp. 84-88, 2010.

[40] T. P. Rao, M. S. Kumar, A. Safarulla, V. Ganesan, S. R. Barman, C. Sanjeeviraja, "Physical properties of ZnO thin films deposited at various substrate temperatures using spray pyrolysis," Physica B: Condensed Matter, vol. 405, no. 9, pp. 2226-2231, 2010.

[41] A. George, "Microstructure and field emission characteristics of ZnO nanoneedles grown by physical vapor deposition," Materials Chemistry and Physics, vol. 123, Art. ID 123-123, 2010.

[42] S. A. Kamaruddin, K. Y. Chan, H. K. Yow, M. Z. Sahdan, H. Saim, D. Knipp, "Zinc oxide films prepared by sol–gel spin coating technique," Applied Physics A: Materials Science & Processing, vol. 104, no. 2, pp. 263-268, 2011.

[43] G. Demircan, S. Yalcin, K. Alivi, G. Ceyhan, M. V. Acikgoz, B. Balak, B. Aktas, R. Das, " The effect of Co and Mn Co-doping on structural and optical properties of ZnO thin films," Optical Materials, vol. 126, pp. 112163, 2022.

[44] M. Abdelkrim, M. Guezzoul, M. Bedrouni, M. Bouslama, A. Ouerdane, B. Kharroubi, " Effect of slight cobalt incorporation on the chemical, structural, morphological, optoelectronic, and photocatalytic properties of ZnO thin film," Journal of Alloys and Compounds, vol. 920, pp. 165703, 2022.

[45] T. K. Pathak, V. Kumar, L. P. Purohit, "High quality nitrogen-doped zinc oxide thin films grown on ITO by sol–gel method," Physica E: Low-Dimensional Systems and Nanostructures, vol. 74, pp. 551-555, 2015.

[46] T. K. Pathak, V. Kumar, H. C. Swart, L. P. Purohit, "Electrical and optical properties of p-type codoped ZnO thin films prepared by spin coating technique," Physica E: Low-Dimensional Systems and Nanostructures, vol. 77, pp. 1-6, 2016.

[47] M. Khan, G. A. Nowsherwan, R. Ali, M. Ahmed, N. Anwar, S. Riaz, A. Farooq, S. S. Hussain, S. Naseem, J. R. Choi, "Investigation of Photoluminescence and Optoelectronics Properties of Transition Metal-Doped ZnO Thin Films," Molecules, vol. 28, 7963, 2023.

[48] A. Faramawy, H. Elsayed, C. Scian, G. Mattei, "Structural, Optical, Magnetic and Electrical Properties of Sputtered ZnO and ZnO:Fe Thin Films: The Role of Deposition Power," Ceramics, vol. 5, pp. 1128-1153, 2022.

[49] Z. Gültekin, M. Alper, C. Akay, M. C. Hacıismailoğlu, "Design and construction of home-made spin coater for OLED production," International Journal of Electronic Devices and Physics, vol. 5, pp. 0-11, 2021.

[50] P. SivaKarthik, V. Thangaraj, S. Kumaresan, K. Vallalperuman, "Comparative study of Co and Ni substituted ZnO nanoparticles: synthesis, structural, optical and photocatalytic activity," Journal of Materials Science:

Materials in Electronics, vol. 28, pp. 10582-10588, 2017.

[51] K. Ravichandran, P. Philominathan, "Comparative Study on Structural and Optical Properties of CdS Films Fabricated by Three Different Low-Cost Techniques," Applied Surface Science, vol. 255, no. 11, pp. 5736-5741, 2009.

[52] R. Karthick, M. Sundararajan, "Design and Implementation of Low Power Testing Using Advanced Razor Based Processor," International Journal of Applied Engineering Research, vol. 12, pp. 6384, 2017.

[53] S. Chattopadhyay, K. P. Misra, A. Agarwala, A. Shahee, S. Jain, N. Halder, A. K. Mukhopadhyay, "Dislocations and particle size governed band gap and ferromagnetic ordering in Ni doped ZnO nanoparticles synthesized via co-precipitation," Ceramics International, vol. 45, no. 17, pp. 23341-23354, 2019.

[54] A. Riaz, A. Ashraf, H. Taimoor, S. Javed, M. A. Akram, M. Islam, K. Saeed, "Photocatalytic and photostability behavior of Ag-and/or Al-Doped ZnO films in methylene blue and rhodamine B under UV-C irradiation," Coatings, vol. 9, no. 3, pp. 202, 2019.

[55] Z. Bazhan, F. E. Ghodsi, J. Mazloom, "The surface wettability and improved electrochemical performance of nanostructured $Co_xFe_{3-x}O_4$ thin film," Surface and Coatings Technology, vol. 309, pp. 554-562, 2017.

[56] C. Ottone, A. Lamberti, M. Fontana, V. Cauda, "Wetting behavior of hierarchical oxide nanostructures: TiO_2 nanotubes from anodic oxidation decorated with ZnO nanostructures," Journal of The Electrochemical Society, vol. 161, no. 10, pp. D484, 2014.

[57] R. Bayati, R. Molaei, A. Richmond, S. Nori, F. Wu, D. Kumar, C. L. Reynolds Jr., "Modification of properties of yttria stabilized zirconia epitaxial thin films by excimer laser annealing," ACS Applied Materials & Interfaces, vol. 6, no. 24, pp. 22316-22325, 2014.

[58] G. J. Chen, S. R. Jian, J. Y. Juang, "Surface analysis and optical properties of Cu-doped ZnO thin films deposited by radio frequency magnetron sputtering," Coatings, vol. 8, no. 8, pp. 266, 2018.

[59] G. Kaur, A. Mitra, K. L. Yadav, "Pulsed laser deposited Al-doped ZnO thin films for optical applications," Progress in Natural Science: Materials International, vol. 25, no. 1, pp. 12-21, 2015.

[60] A. Mahroug, S. Boudjadar, S. Hamrit, L. Guerbous, "Structural, morphological and optical properties of undoped and Co-doped ZnO thin films prepared by sol–gel process," Journal of Materials Science: Materials in Electronics, vol. 25, pp. 4967-4974, 2014.

[61] I. Jellal, O. Daoudi, K. Nouneh, M. Boutamart, S. Briche, M. Fahoume, J. Naja, "Comparative study on the properties of Al-and Ni-doped ZnO nanostructured thin films grown by SILAR technique: Application to solar photocatalysis," Optical and Quantum Electronics, vol. 55, no. 7, pp. 620, 2023.

[62] A. F. Al Naim, A. Solieman, E. R. Shaaban, "Structural, optical, and magnetic properties of Co-doped ZnO nanocrystalline thin films for spintronic devices," Journal of Materials Science: Materials in Electronics, vol. 31, no. 21, pp. 3613-3621, 2020.

[63] P. Mallick, C. Rath, A. Rath, A. Banerjee, N. C. Mishra, "Antiferro to superparamagnetic transition on Mn doping in NiO," Solid State Communications, vol. 150, pp. 29-30, 2010.